14

„Pitfalls“ in the path of quantitative assessment of the severity of oncological lesions in diagnostic nuclear medicine

© A.V. Nesterova,[1,2] N.V. Denisova[1,2]

[1] Novosibirsk State University, Novosibirsk, Russia
[2] Khristianovich Institute of Theoretical and Applied Mechanics, Siberian Branch, Russian Academy of Sciences, Novosibirsk, Russia
e-mail: a.nesterova@g.nsu.ru, nvdenisova2011@mail.ru

Received December 29, 2021
Revised December 29, 2021
Accepted March 2, 2022

When examining patients by single-photon emission computed tomography, the distribution of a radiopharmaceutical drug in biological tissues is evaluated. An active fast-growing tumor has an increased uptake of the drug compared to healthy tissues. In recent years, there has been considerable interest in the level of activity of a radiopharmaceutical in tumor lesions, since it can be useful for monitoring the effectiveness of prescribed therapy. To obtain quantitative results, it is necessary that the applied reconstruction algorithms include the main effects that contribute to the formation of images. One of these factors is the geometric resolution of the collimator. It was expected that taking into account this effect would improve the quantitative assessment of tumor lesions in reconstructed images. However, there were „pitfalls“in the way of obtaining quantitative images. In the diagnostic images obtained taking into account the „geometric resolution of the collimator“, so-called edge artifacts were observed, which manifested themselves in the form of a sharp increase in intensity of radiopharmaceutical accumulation in small tumors and as oscillations in the intensity of radiopharmaceutical accumulation at the edges in large tumors. The problem of edge artifacts casts doubt on the correctness of quantitative assessment the level of intensity of drug accumulation in tumor lesions. In this paper, the problem of edge artifacts is investigated using the method of mathematical modeling. In numerical experiments, the dependence of the quantitative estimate of the intensity of RPD accumulation on the parameters of the reconstruction algorithm was investigated for the first time.

Keywords: Nuclear medicine, mathematical modeling, single-photon emission computed tomography, edge artifacts.

DOI: 10.21883/TP.2022.07.54482.331-21

Introduction

Single-photon emission computed tomography (SPECT) and positron-emission tomography (PET) are modern methods of imaging and diagnostics in the field of medicine. They are based on the detection of radiation of specially developed radiopharmaceutical drugs (RPD). Cancer research uses the drugs whose accumulation in tumors is much higher compared with normal tissues. RPD for SPECT contains a nuclide emitting gamma-quantum during radioactive decay. Gamma ray is usually recorded from different direction using two gamma-ray chamber detectors rotating around the patient's body. Data collected by the detecting system are referred to as „raw“ or input data. Using mathematical methods, input data is transformed into 3D image which describes RPD distribution in the patient's body and analyzed by a radiologist.

Currently, SPECT method is used generally as a semi-quantitative diagnostics method which provides RPD distribution images in relative units. RPD accumulation intensity in the tumor lesion vs. RPD accumulation intensity in the surrounding normal tissues as well as metabolic tumor volume are important predictive indices. Accuracy and reliability of these indices depends on many factors. The research has shown that the tumor lesion images may be distorted due to edge artifacts which appear in case of abrupt transitions of RPD accumulation intensity at image edges. This problem is more essential in cancer research because edge artefacts may cause scintigraphic distortion of tumor lesions on images and unpredictable quantitative estimates of drug accumulation intensity, in particular in small lesions.

To get quantitative values of RPD activity, mathematical reconstruction algorithms shall consider all factors which contribute significantly to generation of SPECT „raw“ data. Geometrical resolution of collimator is an important factor and is described mathematically using point-spread function (PSF). The first statistical iteration reconstruction algorithm generation Maximum Likelihood Expectation Maximization (MLEM) and its accelerated version Ordered Subsets Expectation Maximization (OSEM) did not considered the PSF effect. In recent years, the main tomographic equipment (SPECT and PET) manufacturers have included PSF in OSEM algorithm referred to as Resolution Re-

covery (RR). The PSF consideration was expected to obtain accurate images for quantitative assessment of RPD accumulation. However, „pitfass“ occurred in the effort to obtain accurate quantitative assessments. Diagnostic images with PSF showed so called edge artefacts manifested in the form of sharp growth of PSF accumulation intensity in small tumors compared with calculations without PSF, and PSF accumulation intensity oscillations were observed in large tumors.

Edge artefacts were investigated in previous publications [1,2] reported that high-gradient structure images obtained by emission tomography using a standard MLEM-based approach are highly distorted near the edges of these structures. [3] showed that PSF consideration in MLEM, on the one hand, improved the image resolution and contrast, but on the other hand, caused the edge artefacts on the image and casts doubt on the accuracy of quantitative assessment of small tumor lesions. [4] describes the SPECT/CT research using physical phantom which consisted of a cylinder with six spheres with different diameter simulating the tumor lesions. The phantom image reconstruction was performed using OSEM algorithm. It was shown that the images obtained without PSF consideration had high noise level, and the images with PSF consideration were distorted due to edge effects. Images of large spheres showed edge artefacts in the form of increased RPD accumulation intensity on edges. A surge in RPD accumulation intensity was observed in the center of the images of small spheres. According to the authors of [4], intensities blur together in a single peak on small tumor lesions due to edge artefacts. This ultimately causes quantitative overestimate of RPD accumulation intensity. The investigations in [5] used a specially designed physical phantom. The reconstruction was carried out using OSEM. The test results have shown that reconstruction of images with PSF causes edge artefacts. On larger „lesions“ artefacts were observed in a form of a visible dip in the center and edge artefacts „blur“ together on small „lesions“, which caused quantitative overestimate of RPD accumulation intensity. [6] studied possible SPECT/CT monitoring of chemotherapy response in breast cancer. Initially, phantom investigations were carried out using standard NEMA phantom containing six spheres with different diameters 10, 13, 17, 22, 28, 37 mm. It was noted that an evenly filled 37 mm sphere showed edge artefacts and artefacts may blur together with reduction of sphere diameter causing an increase in the RPD accumulation intensity.

Thus, clinical study and physical material phantom study have shown that PSF consideration in statistical iteration reconstruction algorithms gave erroneous intensities in tumor lesions due to edge artefacts. This is a serious problem since it causes ambiguous interpretation of such images. Edge artefact problem is still unresolved. The research herein uses a mathematical modeling approach for edge artefact study.

1. Statement of the problem. Physical and mathematical model

SPECT examination procedure starts from intravenous injection of special RPD which is a radiolabeled chemical compound. The drug is distributed in the body proportionally to the blood flow. Owing to radioactive decay of isotopes, gamma-quanta are emmitted and recorded by the gamma-ray chamber detector. In traditional clinical practice, two gamma-ray chamber detectors rotate around the patient and collect so called „raw“ data in each sector. In modern SPECT systems, depending on the research objectives, measurements are carried out using 32, 60 and 64 sectors with gamma-ray chamber staying of each of them for 12 to 30 s. „Raw“ measurements obtained from the cameras are used for 3D image reconstruction according to which the conclusion is made.

Physical features of the model:

1. Radioactive decay process is described as follows:

$$n(t) = n(0)e^{-\lambda t} = n(0)e^{-\frac{t}{\tau}},$$

where $n(t) = \{n_j(t)\colon\ j = 1, \ldots, J\}$ is a RPD concentration distribution in a 3D object at time t, $n(0)$ is the initial RPD concentration, λ is the decay constant, τ is the average radioactive atom lifetime.

Technetium-based (^{99m}Tc) drugs are addressed herein. Half-life ^{99m}Tc is 6 h, full raw data acquisition time using the SPECT method Δt may be approx. 30 min. Thus, data acquisition time $\Delta t \ll \tau$, then we may assume that radionuclide concentration in organs remains approximately permanent during acquisition period:

$$n(0 + \Delta t) \approx n(0) - n(0)\frac{\Delta t}{\tau} \approx n(0).$$

Due to spontaneous nature of radiation and low drug concentration, the number of gamma-quanta in all directions in unit time is a random field $f = \{f_j : j = 1, \ldots, J\}$. It is known that this random field is described by the Poisson distribution with mean value proportional to $n(0)$:

$$\bar{f} \approx n(0) - n(0)\left(1 - \frac{\Delta t}{\tau}\right) \approx n(0)\frac{\Delta t}{\tau}.$$

Thus, according to the above assumptions, the average gamma-quanta value emitted from a single volume is considered to be constant during observation and proportional to the local RPD accumulation density.

2. When passing via media with different density, gamma-photon may reach the detector without interaction with the medium substance or may be disseminated or absorbed. Compton scattering and photon photoabsorption are the main types of interaction.

3. For 3D image reconstruction using „raw“ data, the direction of photon arriving to the detector shall be known. In this case, the SPECT model uses a collimator for this. A theoretically ideal collimator allows to obtain an accurate

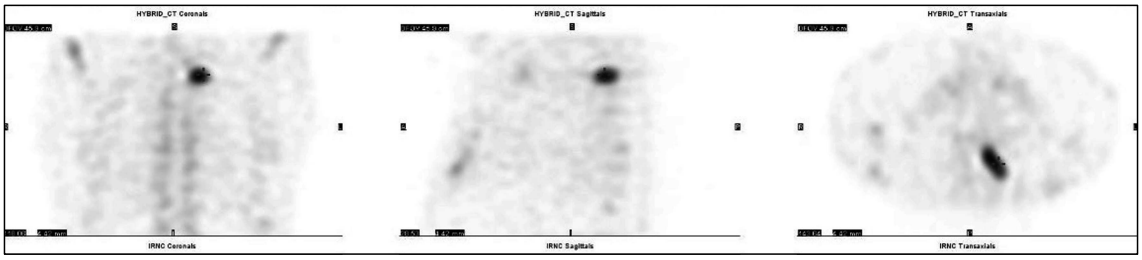

Figure 1. Clinical images obtained during SPECT/CT examination of a patient at the Meshalkin National Medical Research Center (NMITs). ^{99m}Tc-phosphotech was used. A metastatic lesion in a posterior segment of the 3rd rib.

image of a point source. However, real collimators „blur" the point source image with the diameter of the blurred image (spot) increasing with the increase in the distance between the source and collimator surface. The radiation path from the point source via collimator is described by the point-spread function (PSF).

In mathematical formulation, this problem reduces to a system of equations

$$\Sigma_j a_{ij} f_j = g_i \quad \text{or} \quad Af = g,$$

where a_{ij} is a random operator describing the part of gamma-quanta emmitted from the jth voxel which is detected by the ith pixel of the detector.

Here, f_j is the observed Poisson's random variables with unknown mean values $\bar{f}_j$ which are assumed to be proportional to the initial RPD concentration $\bar{f}_j \sim n_j(0)$, and g_i is „raw" data, observed Poisson's random variables with unknown mean values $\bar{g}_i$. These values are associated with the system of linear equations

$$\Sigma_j \bar{a}_{ij} \bar{f}_j = \bar{g}_i, \qquad (1)$$

where $\bar{a}_{ij}$ is the probability that the gamma-quantum emmitted by the jth voxel is recorded by the ith pixel of the detector. Probabilities $\bar{a}_{ij}$ form a system matrix which is assumed to be known. Mathematical problem formulation: using the given $\bar{a}_{ij}$ and g_i, solve the inverse ill-posed recovery problem $\bar{f}_j$ [7].

2. Research methods

Nuclear medicine research involving volunteers or using physical anthropomorphic phantoms has considerable restrictions due to radiation exposure and high research cost. Mathematical modeling method is a worthy alternative. This paper includes mathematical modeling of SPECT examination on the example of a clinical case with a metastatic lesion of thoracic bones. Figure 1 shows diagnostic SPECT images obtained at the Meshalkin National Medical Research Center (NMITs). This research used RPD ^{99m}Tc-phosphotech and a metastatic lesion was detected in a posterior segment of the 3rd rib. The images are presented in frontal, sagittal and axial sections through the tumor lesion.

The modeling procedure was performed step by step closely to clinical study:

1. At the first clinical study stage, RPD ^{99m}Tc-phosphotech was injected to the patient. For mathematical modeling of the SPECT procedure, a simplified mathematical 3D phantom was created to describe ^{99m}Tc-phosphotech distribution in chest organs („virtual patient").
2. At the second clinical study stage, scanning is performed and „raw" input data is acquired using one or two gamma-chamber detectors rotating around the patient. The modeling included calculation of projection data („virtual tomograph").
3. At the third stage, using the measured „raw" input data, a 3D image is obtained using a standard mathematical image reconstruction algorithm Ordered Subsets Expectation Maximization (OSEM). Numerical modeling also used OSEM for image reconstruction.

2.1. Phantom

Diagnostic images in Figure 1 show that ^{99m}Tc-phosphotech is almost evenly distributed in soft tissues, bones and chest organs. A small round area with high RPD capture is clearly visible against this background.

This case was simulated using a simplified mathematical phantom because we wanted to study the edge artefacts in the tumor images. The 3D modeling of the patient's body used an elliptical cylinder with an even background and inserted increased activity ellipsoid simulating the tumor lesion. In numerical experiments, the ellipsoid size — „tumor lesion" — varied. The mathematical phantom is shown in Figure 2.

2.2. „Raw" data calculation („virtual tomograph")

Mathematical modeling of „raw" input data acquisition included the Poisson statistics. The data was calculated by Neumann method using a random number generator. Data calculation metodology and software were previously developed at the Institute of Theoretical and Applied Mechanics, Siberian Branch, Russian Academy of Sciences [7]. Effects of gamma-ray absorption and scattering in biological tissues were not considered herein, because a significant part of the reconstructed area is occupied by lungs and

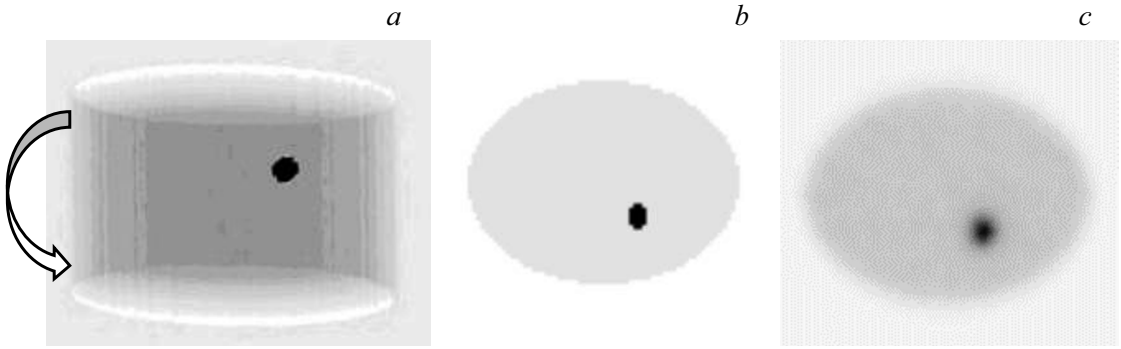

Figure 2. Mathematical modeling of the SPECT examination procedure using RPD ^{99m}Tc-phosphotech. *a* — 3*D* model, the arrow shows the movement of the gamma-chamber detectors; *b* — cross-section through the tumor lesion; *c* — reconstruction of the RPD accumulation intensity distribution in a cross-section through the tumor lesion.

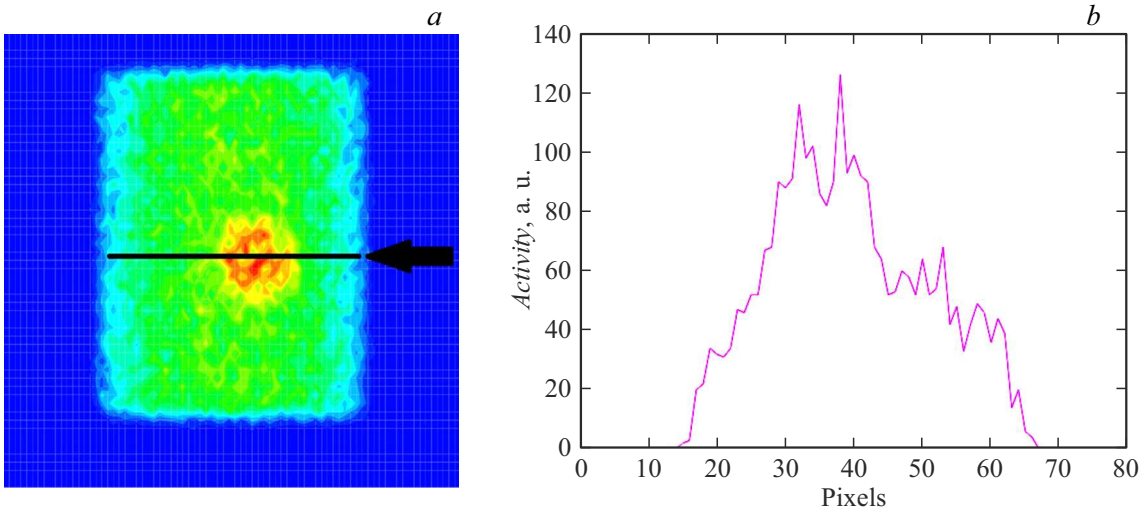

Figure 3. Example of „raw“ input data obtained from one of the angles. *a* — general data view; *b* — example of gamma-quanta distribution along the line through the tumor lesion (shown by the arrow in Figure 3, *a*).

the corresponding cross-sections of gamma-ray interaction in air are small. Gamma-ray passage through the collimator was simulated with PSF consideration using the method described in [8]. Figure 3 shows the example of calculated „raw“ projection data for the developed mathematical phantom obtained from one of the observation angles. Figure 3 shows the example of calculated „raw“ input data for the developed mathematical phantom obtained from one of the observation segments. Figure 3 shows the general view of „raw“ data, Figure 3, *b* shows the gamma-quantum statistics recorded by the detector along the line shown with the arrow in Figure 3, *a*. Stochastic nature of the simulated „raw“ data is clearly visible.

2.3. Image reconstruction

Since the „raw“ input data is of stochastic nature, a statistical approach on the basis of the maximum likelihood method is used to solve the inverse problem of image reconstruction. The image was reconstructed using standard statistical iteration algorithm - OSEM. This algorithm is used on most single-photon emission computed tomographs worldwide.

The measured data has Poisson distribution:

$$P(g|\bar{g}) = e^{-\bar{g}}\frac{\bar{g}^{g}}{g!}.$$

Using equation (1), we get the likelihood function

$$P(g|\bar{f}) = \Pi_i \exp\left(-\Sigma_j \bar{a}_{ij}\bar{f}_j\right)\frac{(\Sigma_j \bar{a}_{ij}\bar{f}_j)^{g_i}}{g_i!}.$$

This approach includes calculation of distribution $\bar{f}$ to maximize the likelihood function $P(g|\bar{f})$:

$$\bar{f}^{*} = arg_{\bar{f}>0}\max P(g|\bar{f}).$$

Finally, the solution (algorithm) is as follows:

$$\tilde{\bar{f}}_j^{n+1} = \frac{\tilde{\bar{f}}_j^{n}}{\Sigma_i \bar{a}_{ij}}\Sigma_i \frac{g_i \bar{a}_{ij}}{\Sigma_j \bar{a}_{ij}\tilde{\bar{f}}_j^{n}}. \quad (2)$$

Expression (2) is the OSEM algorithm [9]. This approach is non-regularized because it does not consider any apriori information, therefore the solution behavior in the iteration process is unstable. As a result of the solution instability, the noise component of the solution is growing with the grow of the number of iterations. Therefore, iteration regularization is used in practice: iteration process is stopped at a predefined iteration and the obtained image is considered as the optimum inverse problem solution. Figure 2, *c* shows phantom reconstruction by OSEM after the second iteration step. RPD accumulation intensity distribution is shown in the cross-section through the „tumor lesion".

The issue of the stop criterion to achieve the optimum image is not solved. For example in nuclear cardiology, for myocardial perfusion by SPECT method, iteration process is stopped in accordance with the established procedure. Shutdown iteration number is determined empirically. In nuclear cardiology, a general shutdown criterion (iteration number) may be established, since most patient have the same cardiac situs and heart size. But in nuclear oncology, such approach is inappropriate, since location and size of tumor lesions in different patients differs significantly.

3. Numerical experiments

Numerical experiments were the first to study the dependence of the quantitative image accuracy of the„tumor lesion" on the reconstruction algorithm parameters and tumor dimensions. A mathematical phantom shown in Figure 2 was used as a „virtual patient" *a, b*. Background activity vs. tumor was 1 : 10. Two tumor lesion sized were addressed: 3 („small tumor") and 6 cm („large tumor"). „Raw" input data was generated using 32 and 60 data acquisition sectors on circular orbit 360° of movement of the gamma-camera detectors with a radius of 25 cm. 3D image reconstruction was performed using standard OSEM algorithm in 2.3. Reconstruction algorithm parameters were set similar to the way by which they may be set for clinical study: 1) iteration process shutdown criterion was set from the 1st to 10th iteration, 2) calculations were carried out with or without PSF consideration in the reconstruction algorithm, 3) calculations were carried with and without solution smoothing. Here, smoothing was performed using median filtering procedure. Image reconstruction was performed in Cartesian coordinate system $\{x, y, z\}$ in the normalized region $\{-1 \le x \le 1;\ -1 \le y \le 1;\ -1 \le z \le 1\}$. Reconstruction area was divided into $80 \times 80 \times 55$ voxels and projection data for 80×55 detectors (pixels) were calculated on each angle. Axis z was oriented along the „patient's body". Figure 2, *c* shows the reconstructed image example. RPD ^{99m}Tc-phosphotech activity distributions are presented in cross-section through the tumor lesion.

3.1. Experiment 1

Model shown in Figure 2 was used in this experiment. A small tumor (3 cm) was simulated. „Raw" data was simulated for 32 sectors. The total number of registered quanta was $9.6 \cdot 10^6$. Dependence of the reconstructed image accuracy of the„tumor lesion" on the reconstruction algorithm variable was studied: 1) iteration process shutdown criterion; 2) PSF consideration the reconstruction algorithm; 3) smoothing filter application.

Figure 4 shows reconstructed profiles going through the „tumor lesions". Each row contains reconstructed „tumor" images depending on the number of iteration process shutdown from 1 to 10. The reconstructed images are overlaid on the precise step-shaped tumor model. The first row contains reconstructed images obtained without PSF and smoothing, the second row contains images with PSF, but without smoothing, the third row contains images without PSF, but with smoothing, and the fourth row contains reconstructed images with PSF and smoothing. Blue curve corresponds to the accurate model profile, red curve corresponds to the reconstructed model profile.

3.2. Experiment 2

In this experiment modeled a large tumor (6 cm). All other conditions were the same as in experiment 1. Figure 5 shows reconstructed profiles going through the „tumor lesions".

3.3. Experiment 3

In this experiment modeled a small tumor (3 cm). As opposed to the previous experiments, „raw" data was simulated for 60 sectors. The total number of registered quanta increased and was $1.8 \cdot 10^7$. Figure 6 shows reconstructed profiles.

3.4. Experiment 4

In this experiment modeled a large tumor (6 cm). „Raw" data was simulated for 60 sectors. All reconstruction parameters were the same as in experiment 3. Figure 7 shows reconstructed activity profiles.

4. Discussion of the results

SPECT method used for cancer patient examination allows to detect tumor lesions, determine the tumor location and approximate scintigraphic dimensions. In recent years, not only tumor detection is of high interest, but also quantitative assessment and determining the RPD accumulation intensity in the tumor lesion. Quantitative SPECT images may be especially useful for monitoring of the allocated therapy performance, because they allow to track quantitative changes at different therapy time stages. In order to obtain precise solutions, the mathematical algorithms used shall consider all effects which contribute to „raw" date generation. One of such effect is the inclusion of the point-spread function in the reconstruction algorithm.

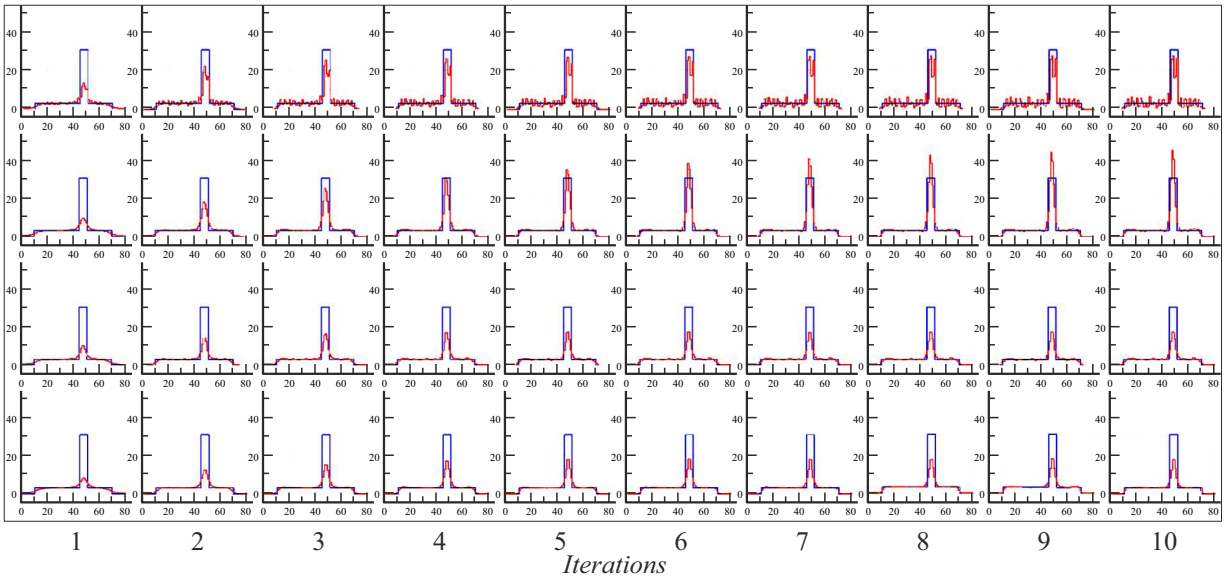

Figure 4. RPD accumulation intensity profiles along the line going through the center of the 3 cm „tumor“ depending on the number of iterations. The reconstruction was carried out using the data obtained from 32 sectors. The first row — reconstruction without PSF, without smoothing, second row — reconstruction with PSF, without smoothing, third row — reconstruction without PSF, with smoothing, fourth row — reconstruction with PSF, with smoothing. Blue curve (online version) corresponds to the accurate model profile, red curve (online version) corresponds to the reconstructed model profile.

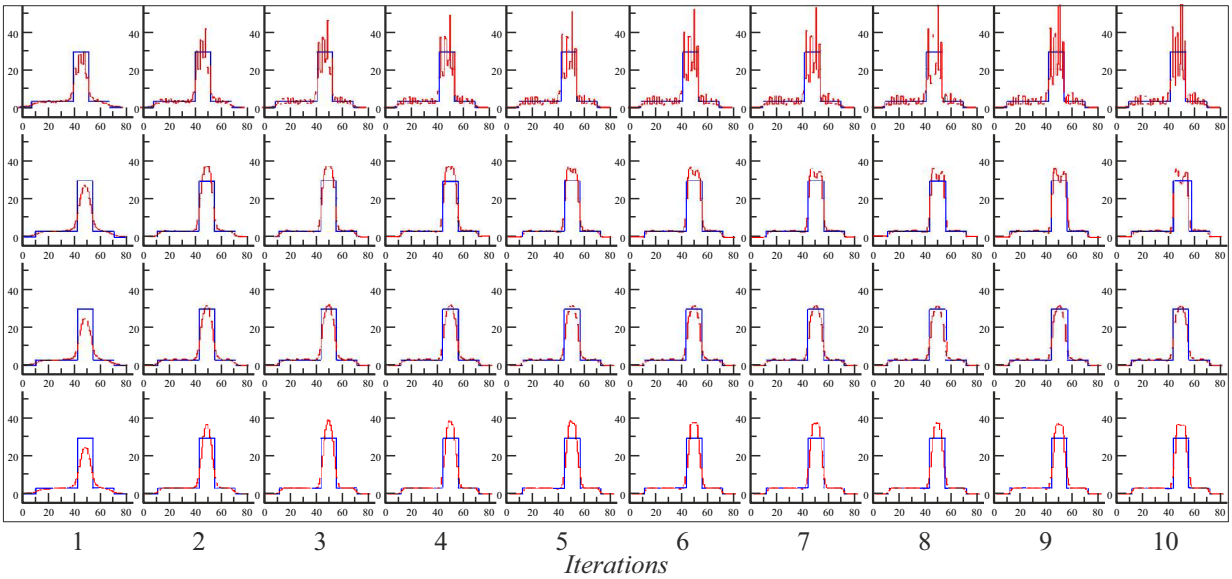

Figure 5. RPD accumulation intensity profiles along the line going through the center of the 6 cm „tumor“ depending on the number of iterations. The reconstruction was carried out using the data obtained from 32 sectors. The first row — reconstruction without PSF, without smoothing, second row — reconstruction with PSF, without smoothing, third row — reconstruction without PSF, with smoothing, fourth row — reconstruction with PSF, with smoothing. Blue curve (online version) corresponds to the accurate model profile, red curve (online version) corresponds to the reconstructed model.

Results of reconstruction without PSF for small and large tumor lesions shown in the first row in Figures 4 and 5 demonstrate very noisy solutions which cannot be used for quantitative assessment. For the small tumor, the image contains one or two peaks, and for the large tumor, reconstructed image in the profile is comb-shaped. Increase in the number of data acquisition angle somehow improves the solution (the first row in Figures 6 and 7), but does not solve the problem of good quantitative solution.

PSF introduction into OSEM reconstruction algorithm shall improve the quantitative solution. However, edge artefacts appeared on the obtained images. The edge

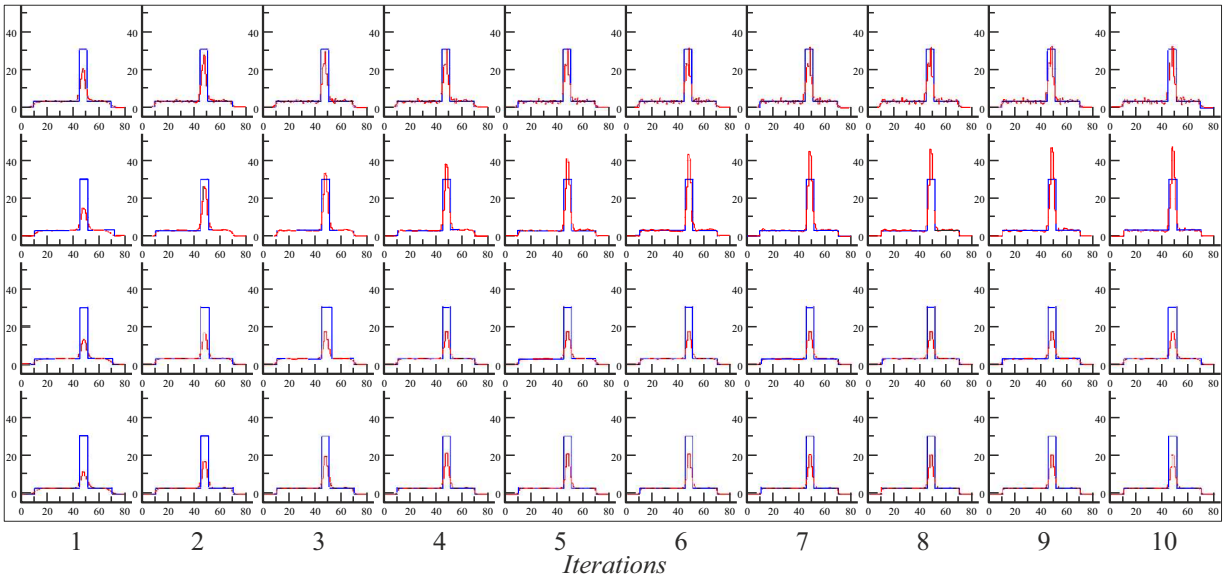

Figure 6. RPD accumulation intensity profiles along the line going through the center of the 3 cm „tumor" depending on the number of iterations. The reconstruction was carried out using the data obtained from 60 sectors. The first row — reconstruction without PSF, without smoothing, second row — reconstruction with PSF, without smoothing, third row — reconstruction without PSF, with smoothing, fourth row — reconstruction with PSF, with smoothing. Blue curve (online version) corresponds to the accurate model profile, red curve (online version) corresponds to the reconstructed model.

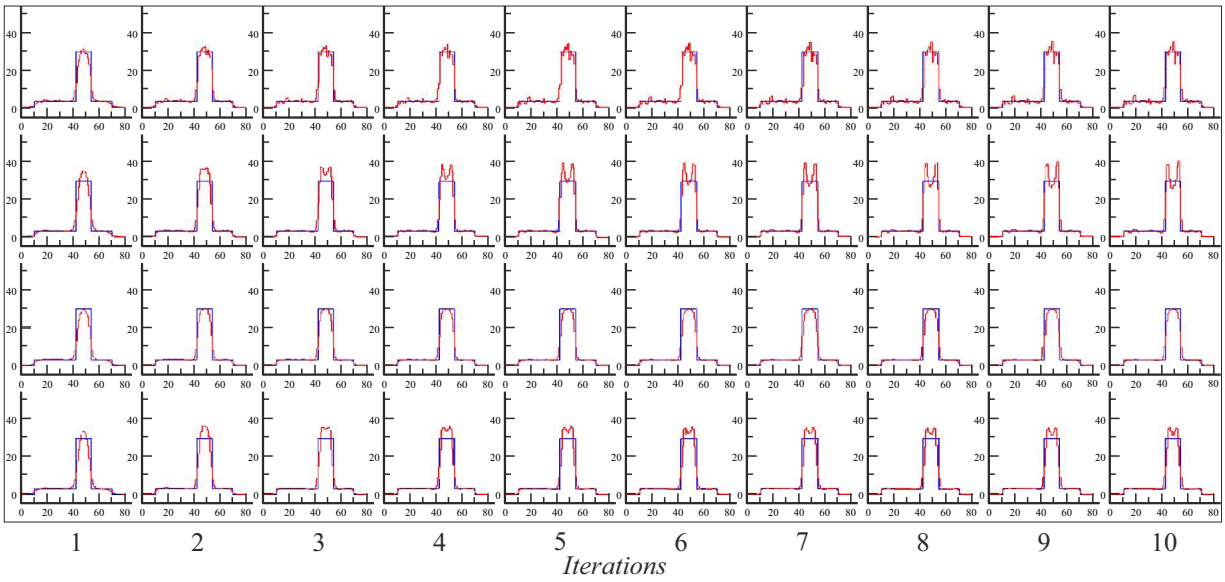

Figure 7. RPD accumulation intensity profiles along the line going through the center of the 6 cm „tumor" depending on the number of iterations. The reconstruction was carried out using the data obtained from 60 sectors. The first row — reconstruction without PSF, without smoothing, second row — reconstruction with PSF, without smoothing, third row — reconstruction without PSF, with smoothing, fourth row — reconstruction with PSF, with smoothing.

artefacts are clearly seen on all reconstructed images shown in the second raw in Figure 4–7 which manifested themselves in surge of the RPD accumulation intensity in small tumors and intensity growth was observed at the tumor lesion edges in large tumors. These results correspond to the experimental measurements carried out using physical phantoms [3,5]. The edge artefact problem casts doubt on the correctness of quantitative assessment of the RPD accumulation intensity on the tumor lesion images. An odd situation occurred when PSF inclusion in the reconstruction algorithm causes ambiguous images. In order to overcome the edge artefact problem, some authors offered to use image smoothing using various filtration methods [10]. The images in the third row in Figures 4–7 obtained without

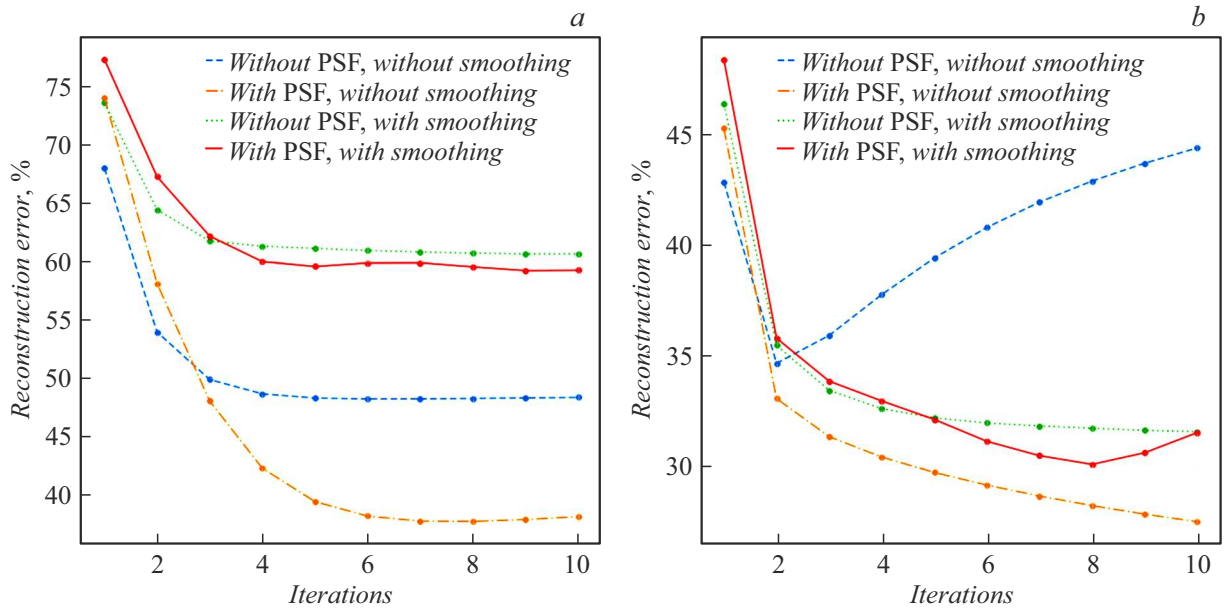

Figure 8. Dependence of RMS error for 3 cm(a) and 6 cm (b) tumors.

PSF, but with smoothing show wrong quantitative values of PSF accumulation intensity for small tumor. For large tumor lesions, smoothing improves the images, however, the reconstructed profile diameter is lower than that of the precise phantom profile. The last row in Figure 4−7 contains the images with PSF and smoothing. As shown in these figures, for small tumors, smoothing completely masks the PSF effect, while the images with smoothing, with and without PSF look similarly wrong. For large tumor lesions, PSF consideration causes edge artefacts. Visual analysis of profiles shown in Figure 4−7 does not provide a definite answer regarding the benefits of the images obtained with PSF compared with images without PSF. For quantitative assessment of reconstructed images of tumor lesions, RMS error of reconstruction was calculated Δ:

$$\Delta = \frac{\sqrt{\Sigma_{i,j,k}\left(f(i,j,k) - \overline{f}_n(i,j,k)\right)^2}}{\sqrt{\Sigma_{i,j,k}\left(f(i,j,k)\right)^2}},$$

where (i, j, k) are pixel coordinates, f is the function of the exact model, $\overline{f}_n$ is the function of the reconstructed model.

Figure 8 shows the reconstruction error dependence for the numerical experiments.

Figure 8 shows that for a 3 cm small tumor, the minimum error is achieved during image reconstruction with PSF, without smoothing, while the maximum error was obtained for reconstruction without PSF using median filtration. For 6 cm tumor in Figure 8, b, the minimum error is achieved similarly during image reconstruction with PSF, without smoothing, and the maximum error is observed during reconstruction without PSF and without median filtration. Thus, regardless of the tumor size, quantitative assessment of the image reconstruction shows that a more correct image will be obtained by reconstruction with PSF, without filtration. This result is consistent with the author's opinion [11] which says that the use of filtration for edge artefact smoothing during reconstruction with PSF contradicts the purpose of PSF introduction in OSEM. Filtration deteriorates the image resolution while PSF is introduced specifically to improve this quality.

Conclusion

Precise quantitative assessment of the RPD accumulation intensity in tumor lesions is an important objective in diagnostic nuclear medicine, because it opens opportunities for therapy efficiency monitoring. The mathematical modeling research herein showed that geometrical resolution of the collimator described in the form of point-spread function shall be considered for quantitative assessment of the RPD accumulation intensity assessment. However, PSF introduction in the reconstruction algorithm causes edge artefacts in tumor lesion images. According to the obtained simulation results, a conclusion may be made that standard OSEM algorithm does not cope with the edge artefact problem. Smoothing does not solve the problem and causes the increase in reconstruction error. Investigations shall be made using new-generation statistical algorithms based on Maximum a Posteriori Bayesian method.

Conflict of interest

The authors declare that they have no conflict of interest.

References

[1] D.L. Snyder, M.I. Miller, L.J. Thomas, D.G. Politte. IEEE Tr. Med. Imaging, **6** (3), 228–238 (1987). DOI: 10.1109/TMI.1987.4307831
[2] D.G. Politte, D.L. Snyder. IEEE Tr. Nucl. Sci., **35** (1), 608–610 (1988). DOI: 10.1109/23.12796
[3] A. Rahmim, J. Qi, V. Sossi. Med. Phys., **40** (6), 064301 (2013). DOI: 10.1118/1.4800806
[4] T. Kangasmaa, A. Sohlberg, J.T. Kuikka. Int. J. Mol. Imaging, **2011** (3), 630813 (2011). DOI: 10.1155/2011/630813
[5] Y. Tsutsui, S. Awamoto, K. Himuro, Y. Umezu, S. Baba, M. Sasaki. Asia Ocean J. Nucl. Med. Biol., **5** (2), 134–143 (2017). DOI: 10.22038/aojnmb.2017.8802
[6] A. Collarino, L.M. Pereira Arias-Bouda, R.A. Valdés Olmos, P. van der Tol, P. Dibbets-Schneider, L.-F. de Geus-Oei, F.H.P. van Velden. Med. Phys., **45** (5), 2143–2153 (2018). DOI: 10.1002/mp.12880
[7] N.V. Denisova, I.N. Terekhov Med. fizika **3**, 32–39 (in Russian).
[8] A.R. Formiconi. Phys. Med. Biol., **43** (11), 3359–3379 (1998). DOI: 10.1088/0031-9155/43/11/013
[9] K. Lange, E. Carson. J. Comput. Assist. Tomogr., **8** (2), 306–316 (1984).
[10] I.S. Armstrong, M.D. Kelly, H.A. Williams, J.C. Matthews. EJNMMI Phys., **1**, 99 (2014). DOI: 10.1186/s40658-014-0099-3
[11] J. Nuyts. EJNMMI Phys., **1**, 98 (2014). DOI: 10.1186/s40658-014-0098-4